SISSA

Cluster ions in gas-based detectors

View the article online for updates and enhancements.

You may also like

- Models of granular ratchets
  G Costantini, A Puglisi and U Marini
  Bettolo Marconi

- The hypergeometric series for the partition
  function of the 2D Ising model
  G M Viswanathan

- Quantum geometry of three-dimensional
  lattices
  Vladimir V Bazhanov, Vladimir V
  Mangazeev and Sergey M Sergeev

Cluster ions in gas-based detectors

Y. Kalkan,[a,b,1] **M. Arslandok,**[c] **A.F.V. Cortez,**[d] **Y. Kaya,**[e] **İ. Tapan**[a] **and R. Veenhof**[f,a]

[a]*Department of Physics, Uludağ University,*
 16059 Bursa, Turkey

[b]*Department of Physics, Muş Alparslan University,*
 49250 Muş, Turkey

[c]*Institut für Kernphysik, Goethe-Universität,*
 Max-von-Laue-Straße 1, 60438 Frankfurt am Main, Germany

[d]*Laboratório de Instrumentação e Física Experimental de Partículas – LIP,*
 Departamento de Física, Faculdade de Ciências e Tecnologia, Universidade de Coimbra,
 Rua Larga, 3004-516 Coimbra, Portugal

[e]*Department of Chemistry, Uludağ University,*
 16059 Bursa, Turkey

[f]*RD51 collaboration, CERN,*
 Genève, Switzerland

E-mail: yalcinkalkan@gmail.com

ABSTRACT: Avalanches in gas-based detectors operating at atmospheric pressure and using Ar-CO_2 or Ne-CO_2 as drift medium produce in a first instance mainly Ar^+, Ne^+ and CO_2^+ ions. The noble gas ions transfer their charge to CO_2 in a few ns. A few ns later, the CO_2^+ ions have picked up CO_2 molecules, forming cluster ions, in particular $CO_2^+ \cdot (CO_2)_n$. Since the cluster ions are slower than the initial ions, the signals induced by ion motion are altered. The effect is shown to be present in constant-field detectors and TPC readout chambers, and is expected to affect devices such as Micromegas and drift tubes.

---

[1]Corresponding author.

Contents

1 Introduction

1.1 Cluster ions

Cluster ions consist of a core ion and one or more neutral atoms and molecules. They are held together by the attractive force between the ion charge and the (induced) dipoles. Their binding energy, typically $0.1 - 1.5\,\text{eV}$, is in-between that of chemically bound molecules and van der Waals molecules. Formation of $CO_2^+ \cdot CO_2$ clusters has a particularly large rate constant and these clusters should be abundant in mixtures quenched by CO_2.

1.2 Overview

Although there is a wealth of information in the literature about ion transport and ion chemistry, some gas-detector simulations simplify the treatment of ions to excess, e.g. by taking only the noble gas ions into account, neglecting the role of the quencher. Such calculations happen to be in fair agreement with measurements (section 4.3), but the approach is unphysical because Ar^+ and Ne^+ ions transfer their charge to CO_2 in a few ns (section 2.2).

Section 2 explains how $CO_2^+ \cdot CO_2$ becomes the dominant ion species after a few tens of ns at atmospheric pressure. These clusters grow to become $CO_2^+ \cdot (CO_2)_n$. The ion core may change, but clusters dominate for at least a few hundred μs. Section 3 reviews the literature on the mobility of ions and cluster ions. Section 4 shows how cluster ions manifest themselves in detectors, illustrating this with the mobility of signal ions in uniform fields and in TPC readout chambers.
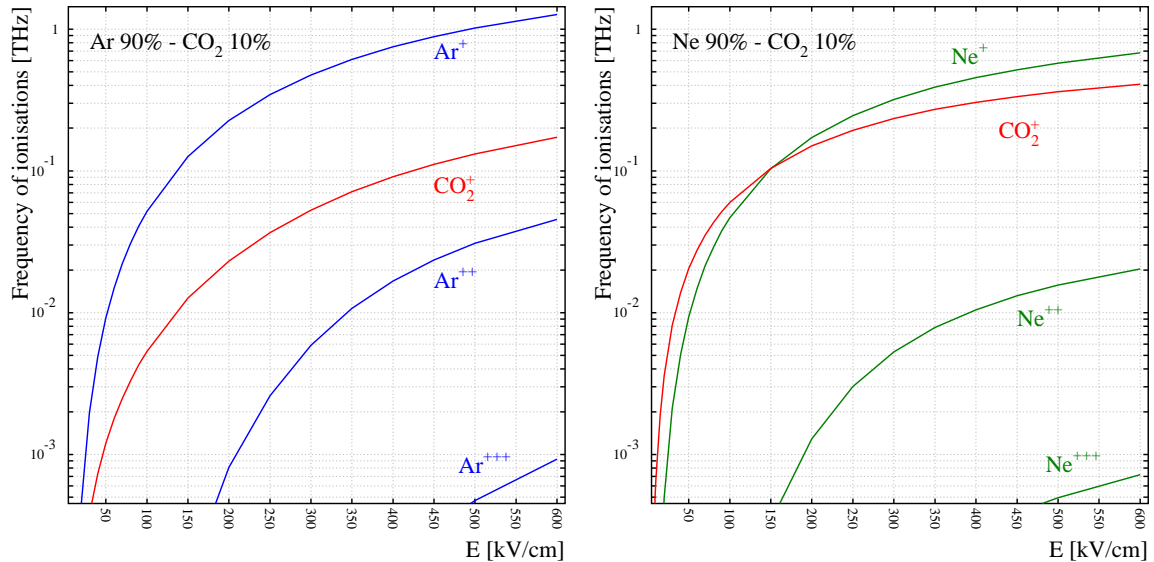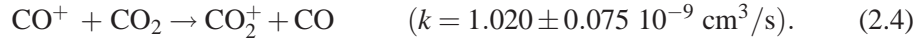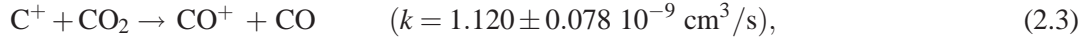
2 Cluster ion formation

2.1 Avalanche

Figure 1. Ionisation rates in Ar 90%-CO_2 10% (*left*) and Ne 90%-CO_2 10% (*right*). Calculated using Magboltz version 10.6 [8, 63].

Avalanches in Ar-CO_2 at atmospheric pressure and room temperature initially produce Ar^+ ions and a lesser quantity of ions derived from CO_2. Ne-CO_2 mixtures generate comparatively fewer Ne^+ ions owing to the higher ionisation potential of Ne, see figure 1.

Ionisation of the noble gases is straightforward — multiple ionisation and ionisation of the inner shells play no significant role. In contrast, bombarding CO_2 with $20-100\,eV$ electrons produces, depending on pressure, a range of ions as shown by H.W. Ellis et al. [16]. At $0.013\,Pa$, CO_2^+ makes up 98% of the ions, but traces of C^+, O^+ and CO^+ are also observed. These are not anymore seen at $0.13\,Pa$. O_2^+ ions start to emerge at $0.26\,Pa$ and their abundance rises steadily with pressure.

Their origin has been the subject of much debate since they seems to be more common than can be accounted for by reaction (2.2) alone [66]. At 8 Pa, larger ions, including the first clusters, appear and at 100 Pa the most common ions (98% of the total) are O_2^+ and $O_2^+ \cdot CO_2$.

These trace ions are probably also produced at atmospheric pressure, but not observed because they react rapidly with CO_2 (rate constants are weighted averages of values taken from [3, 69]):

$$O^+ + CO_2 \rightarrow O_2^+ + CO \qquad (k = 1.03 \pm 0.10 \ 10^{-9} \ \mathrm{cm^3/s}), \tag{2.1}$$

$$O_2^+ + CO_2 + M \rightarrow O_2^+ \cdot CO_2 + M \qquad (k = 0.5 \pm 0.1 \ 10^{-30} \ \mathrm{cm^6/s}), \tag{2.2}$$

$$C^+ + CO_2 \rightarrow CO^+ + CO \qquad (k = 1.120 \pm 0.078 \ 10^{-9} \ \mathrm{cm^3/s}), \tag{2.3}$$

$$CO^+ + CO_2 \rightarrow CO_2^+ + CO \qquad (k = 1.020 \pm 0.075 \ 10^{-9} \ \mathrm{cm^3/s}). \tag{2.4}$$
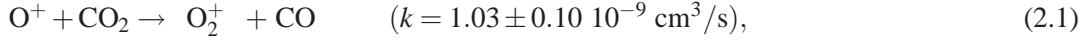
At atmospheric pressure and in a mixture with 10% CO_2, the two-body reaction times[1] are around 370 ps. O_2^+ ions form clusters with CO_2 molecules in a three-body reaction. Excess kinetic and binding energy is evacuated by a "helper" molecule M. This takes 300 ns if only CO_2 acts as helper and is 10 times faster if all gas molecules take part. Only the cluster, and maybe O_2^+, will therefore be detectable at atmospheric pressure.

2.2 Reactions of argon and neon ions

Argon has a higher ionisation potential than CO_2 and Ar^+ ions transfer their charge to CO_2 molecules in ~ 0.85 ns assuming 10% CO_2 [4]:

$$Ar^+ + CO_2 \rightarrow Ar + CO_2^+ \qquad \left(k = 4.80 \pm 0.72 \ 10^{-10} \ \mathrm{cm^3/s}\right). \tag{2.5}$$
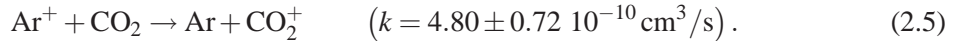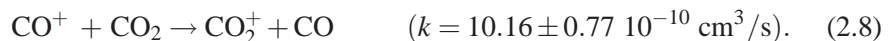
Alternatively, Ar^+ ions can form molecular ions, as reported already in 1951 by John Hornbeck [29]. He attributed this to homonuclear associative ionisation, a two-body process. At higher pressure, they can also be formed in a three-body interaction:

$$Ar^+ + Ar + M \rightarrow Ar^+ \cdot Ar + M \qquad \left(k = 2.3 \pm 0.2 \ 10^{-31} \ \mathrm{cm^6/s}\right) \tag{2.6}$$
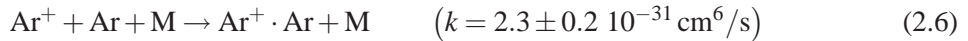
where M, either Ar or CO_2, ensures energy-momentum is conserved. The rate constant is taken from Wei-cheng F. Liu and D.C. Conway [43]. A similar value $k = 2.0 \ 10^{-31} \ \mathrm{cm^6/s}$ was published by K. Hiraoka and T. Mori [26]. B.M. Smirnov [69] recommends $k = 2.2 \ 10^{-31} \ \mathrm{cm^6/s}$. As pointed out in [43], only $^2P_{3/2}^o$ associates at room temperature — $^2P_{1/2}^o$ only does so at lower temperatures. In a mixture with 90% Ar where only Ar acts as helper, the reaction takes 8.9 ± 0.8 ns.

Resonant charge exchange of Ar^+ with Ar has a rate constant $k = 4.6 \ 10^{-10} \ \mathrm{cm^3/s}$ [44] and thus a reaction time of 100 ps — much faster than molecular ion formation. However, for our purposes, this reaction is important only in that it dramatically lowers the mobility of Ar^+ in Ar. The same happens to Ne^+ in Ne, see section 3.4.

In Ne mixtures, charge transfer is a 2-step reaction which takes ~ 8 ns assuming 10% CO_2:

$$Ne^+ + CO_2 \rightarrow CO^+ + O + Ne \qquad (k = 0.500 \pm 0.050 \ 10^{-10} \ \mathrm{cm^3/s}), \tag{2.7}$$

$$CO^+ + CO_2 \rightarrow CO_2^+ + CO \qquad (k = 10.16 \pm 0.77 \ 10^{-10} \ \mathrm{cm^3/s}). \tag{2.8}$$

---

[1]Reaction times, written τ, are to be understood as the time after which a fraction $1/e$ of the reactant remains. These times have been derived from the rate constants assuming a number density at room temperature $N = 2.45 \ 10^{19}/\mathrm{cm^3}$.

The CO_2^+ ions go on to form clusters as described in section 2.3. The rate constants cited above are (weighted averages of) values from the compilation of V.G. Anicich and W.T. Huntress Jr. [3].

Clustering is slower in Ne than in Ar [69]:

$$Ne^+ + Ne + M \rightarrow Ne^+ \cdot Ne + M \qquad \left(k = 0.6 \ 10^{-31} \ cm^6/s\right). \tag{2.9}$$
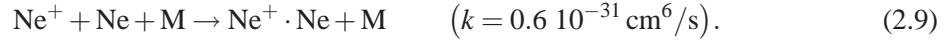
2.3 Reactions of carbon dioxide ions

For our purposes the most important reaction of CO_2^+ is three-body association with CO_2 resulting in $CO_2^+ \cdot CO_2$ cluster ions:

$$CO_2^+ + CO_2 + M \rightarrow CO_2^+ \cdot CO_2 + M. \tag{2.10}$$

The compilation of B.M. Smirnov [69] gives a rate constant for this reaction of $k = 2.4 \ 10^{-28} \ cm^6/s$, close to the value $k = 2.1 \ 10^{-28} \ cm^6/s$ cited by A.B. Rakshit and P. Warneck [58]. P. Coxon and J.L. Moruzzi have measured a forward rate constant $k = 0.8 \pm 0.2 \ 10^{-28} \ cm^6/s$ and an electric field dependent backward rate constant $k = 10^{-14} - 10^{-11} \ cm^3/s$ [11].

If only CO_2 acts as helper, and assuming there is 10% CO_2 in the gas mixture, then the characteristic time for cluster formation is $0.7 - 2.0 \, ns$. The reaction is 100 times faster if also Ar acts as helper. Association, even in mixtures containing little CO_2, is therefore substantially faster than ion transit in gas-based detectors, which is typically in the range $100 \, ns - 100 \, \mu s$.

CO_2^+ is also reported to undergo two-body association with argon, resulting in an excited intermediate state, after which CO_2 is substituted for Ar [35], thus producing the same $CO_2^+ \cdot CO_2$ cluster. The rate constants for this mechanism are not known:

$$CO_2^+ + Ar \rightarrow CO_2^+ \cdot Ar, \tag{2.11}$$

$$CO_2^+ \cdot Ar \ + CO_2 \rightarrow CO_2^+ \cdot CO_2 + Ar. \tag{2.12}$$
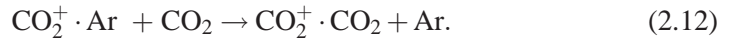
Resonant charge exchange in pure CO_2 has a time scale of $\sim 110 \, ps$ [4], considerably longer than the $7 - 20 \, ps$ needed for three-body association in pure CO_2. The effect on the mobility is therefore minor compared to the noble gases, see figures 4 and 5:

$$CO_2^+ + CO_2 \rightarrow CO_2 + CO_2^+ \qquad \left(k = 3.70 \pm 0.37 \ 10^{-10} \ cm^3/s\right). \tag{2.13}$$

2.4 Initial clusters in argon-carbon dioxide mixtures

The documented cluster-forming reactions are shown in red in figure 2 (left). The most likely outcome is $CO_2^+ \cdot CO_2$, even when starting from Ar^+. Formation of the $Ar^+ \cdot Ar$ dimer is, except at high Ar fractions and at pressures far above atmospheric, overshadowed by the charge exchange reaction (2.5), as shown by figure 2 (right).

Of the non-established reactions, only the pathway $Ar^+ - Ar^+ \cdot CO_2 - Ar^+ \cdot Ar$ produces Ar dimers. The first step, masked by the inter-molecular charge exchange reaction (2.5), is encouraged by the higher polarisability of CO_2 but hampered by the higher stability of $Ar^+ \cdot Ar$. The ligand switch in the second step benefits from the higher binding energy of homonuclear clusters, as discussed by A. Illies et al. [35], but it is dubious whether this can compete with the intra-cluster charge exchange from $Ar^+ \cdot CO_2$ to $Ar \cdot CO_2^+$. Although no information was found in the literature regarding this reaction, there is little doubt it is fast due to the lower ionisation potential of CO_2.
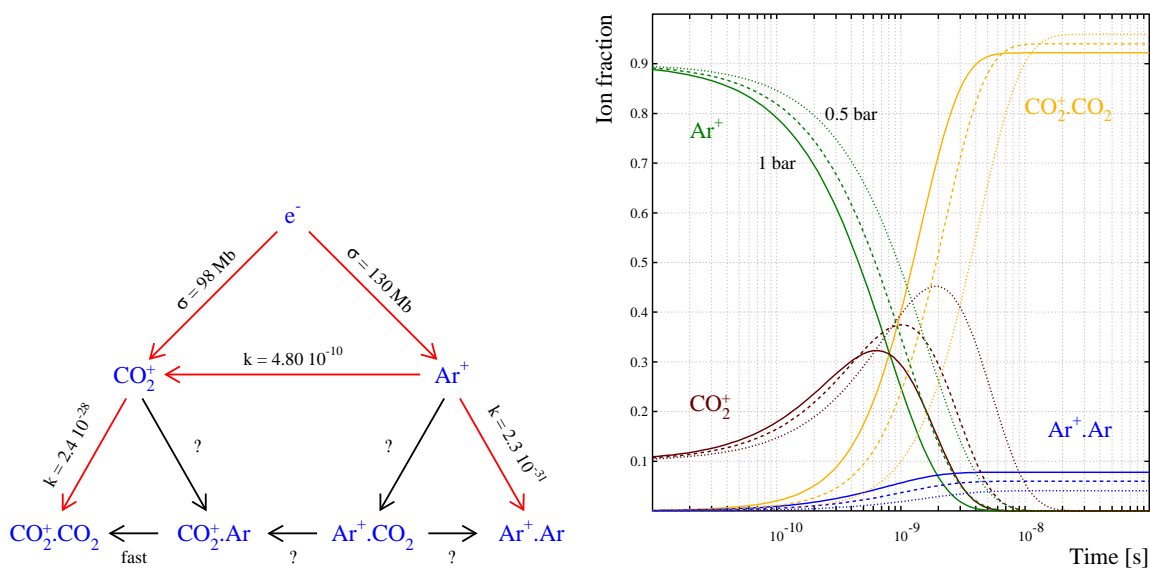
Figure 2. *Left*: diagram of the formation of clusters in Ar-CO_2 mixtures and subsequent transitions. Known transitions are shown in red. Rate constants in units of cm^3/s or cm^6/s as appropriate. *Right*: resulting evolution of the ion and cluster count. Ar^+ make up 90% of the initial ions. Most of these transfer their charge to CO_2^+, especially at lower pressures. The CO_2^+ ions go on to form clusters with CO_2 molecules. Gas pressures are 1 bar (solid), 0.75 bar (dashed) and 0.5 bar (dotted). Calculated from the rate constants, using Mathematica [73].

2.5 Cluster growth and decay

According to van 't Hoff diagrams for $CO_2^+ \cdot (CO_2)_n$ clusters [27, 34], $CO_2^+ \cdot CO_2$ does not grow further at 300 K and low pressure (70 – 400 Pa). The same applies to $Ar^+ \cdot (Ar)_n$ clusters [26, 71].

At higher pressure, the clusters become larger as shown by two experiments at atmospheric pressure and room temperature. The positive ion mass spectrum of H.W. Ellis et al. [16] can be interpreted as an HCO^+ ion core surrounded by nCO_2 where $n = 2 - 8$. The hydrogen atom stems from an air contamination. In an analysis of this data, Z. Berant et al. [7] found that the cluster size could be $n \approx 4.3$. Z. Berant et al. have also shown for a set of 18 molecules with a mass in the range 46 – 522 Da that $n \propto \exp(-T_0/T)$ at temperatures in the range 90 – 250 °C. Extrapolating to room temperature would yield a considerably larger size ($n \approx 12$).

Y. Ikezoe et al. [33] have observed two families of clusters: $CO_2^+ \cdot (CO_2)_n$ ($n = 0 - 4$) and $CO^+ \cdot (CO_2)_n$ ($n = 2, 3$) during the first 200 μs. These clusters are formed in the first 100 μs and disappear with a (common) time constant of 190 μs. From 200 μs onwards, these clusters are no longer observed. Instead other families of clusters emerge. All of these contain H_2O, CO or both.

In line with their rapid formation, $CO_2^+ \cdot CO_2$ clusters have a large enthalpy of formation 0.68 ± 0.04 eV [47] and may therefore be expected to have a long lifetime. The enthalpy for adding further CO_2 molecules progressively decreases [27]. In the light of the findings of Y. Ikezoe et al. and P.C. Engelking [20], it seems safe to assume that the lifetime of $CO_2^+ \cdot CO_2$ is measured at least in tens or hundreds of μs. Cluster dissociation is therefore not a significant source of CO_2^+. The lifetime of the $Ar^+ \cdot Ar_n$ molecular ion depends on the cluster size, and is in the range of 60 – 75 μs [40].

3 Mobility

3.1 Blanc's law

Blanc's law [10] provides a simple method to compute the mobility of an ion in a mixture of gases. It states that the reciprocal of the mobility in a mixture equals the weighted sum of the reciprocals in the pure components.

The formula can be found by separating the mixture and making the ion successively traverse each component. The total time needed is $\sum_i d_i(E/K_i)$ where the d_i are the thicknesses of the gas layers. Blanc's law states that this equals $d(E/K_{\mathrm{mix}})$ where $d = \sum_i d_i$ and K_{mix} the mobility in the mixed gases. The law can not be expected to hold if the component gases react between them. Similarly, when the ion forms clusters with the carrier gas, deviations are to be expected.

T. Holstein has shown [9, 28] that departures from Blanc's law are otherwise always positive and of the same magnitude as the higher order corrections on the mobilities of the ingredients. This is explained in more detail by Stanley I. Sandler and E.A. Mason [64]. These authors list cases where Blanc's law is expected to be least accurate, such as a light polar gas mixed with a heavy gas, for which the error reaches $\sim 5\%$. Our gases have no permanent dipole but the lowest vibration modes of CO_2, the $80\,\mathrm{meV}$ bending modes, are 4.5% populated at room temperature. These oscillating dipoles have weak London-like interactions with other gas molecules. Also the quadrupole moment of CO_2 generates only a minor force. Hence, Blanc's law should for our purposes be accurate to a few percent.
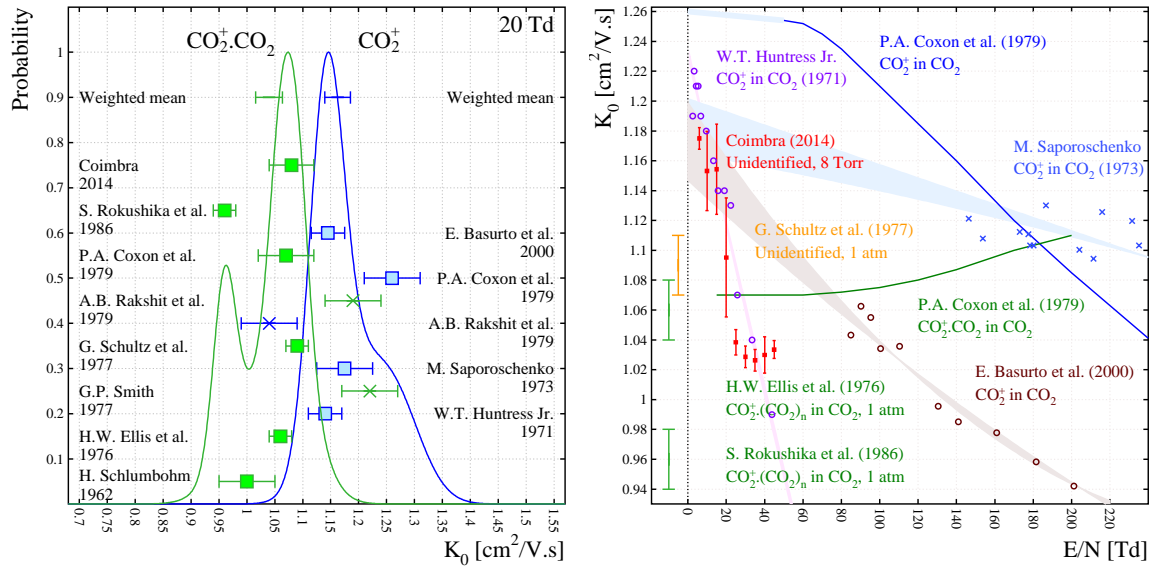

Figure 3. *Left*: profile of measurements of the reduced mobility of CO_2^+ and $CO_2^+ \cdot (CO_2)_n$ ions in CO_2. G. Schultz et al. [68] and P.M.C.C. Encarnação et al. [19], although purporting to have measured the ion, almost certainly measured a cluster. The measurements of A.B. Rakshit and P. Warneck [58] and of G.P. Smith [70] have not been included in the weighted averages — see the text. Estimated errors have been used where the original publication states no uncertainty. Inaccurate extrapolations have been corrected in a few cases. *Right*: E/N graphs for some of the mobility measurements. Data shown in red and orange was taken without mass spectrometry. Due to poor image quality, some data points may be missing or shifted.

3.2 Carbon dioxide ions in their parent gas

Measuring the mobility of CO_2^+ in CO_2 is fraught with difficulties: CO_2^+ forms clusters with its parent gas, with contaminants like water and with parasitically produced oxygen [16]. Experiments without mass spectrometry can not distinguish CO_2^+ from clusters and the mobility computed from the Langevin formula in the polarisation limit ($\sim 1.8 \, cm^2/V.s$) is not accurate, see section 3.4.

The mobility was first measured in 1971 by W.T. Huntress Jr. at pressures below 1 Pa. He obtained a zero-field mobility of $1.21 \pm 0.02 \, cm^2/V.s$ [31]. This was confirmed in 1979 by P.A. Coxon and J.L. Moruzzi who found $1.26 \pm 0.05 \, cm^2/V.s$ at $p = 3.5 - 13 \, Pa$ [12]. This measurement has been adopted in the compilation of L.A. Viehland and E.A. Mason [72]. Both experiments were particularly careful with the purity of their gas. M. Saporoschenko [65] has reported data for $E/N > 140 \, Td$ at 77 Pa, but this can not accurately be extrapolated to the 20 Td fields that we need, see figure 3 (right). In addition, this measurement has been criticised for its potential oxygen contamination. More recently, E. Basurto et al. [5] have measured the mobility at $p = 0.66 - 20 \, Pa$ and room temperature. These measurements cover $E/N > 85 \, Td$ and hence require less extrapolation than the data of M. Saporoschenko.

Even though the mobilities of these four experiments agree to an extent when extrapolated to low field, the E/N dependencies differ, see figure 3 (right).

A publication by A.B. Rakshit and P. Warneck [58], although primarily concerned with rate coefficients, contains values for the ion and cluster ion mobilities at low pressure. Their values are puzzling in that they seem to have been interchanged.

3.3 Carbon dioxide cluster ions in carbon dioxide

P.A. Coxon and J.L. Moruzzi identified the $n = 1$ cluster at $p = 53 - 67 \, Pa$ alongside the ion [12]. Their low-field result $1.07 \pm 0.04 \, cm^2/V.s$ has been adopted in compilation [72].

Both S. Rokushika et al. [61] and H.W. Ellis et al. [16] have observed that all positive clusters have approximately the same mobility at atmospheric pressure. CO_2 readily forms large clusters owing to its polarisability, and the precise nature of the ion core plays only a minor role. One may speculate that the clusters repeatedly pick up and shed CO_2 molecules during their transit in the apparatus. As a result, the mass of a cluster measured in the mass spectrometer is not necessarily the mass that the cluster had when its mobility was measured. Even though the experiments worked at the same pressure and temperature, they did not find the same mobility: $0.96 \pm 0.02 \, cm^2/V.s$ respectively $1.06 \pm 0.02 \, cm^2/V.s$. The authors suggest this could be related to contamination.

For lack of mass spectrometry, G. Schultz et al. [68] did not attempt to identify the ions, but considering that they worked at atmospheric pressure, it is probable they observed a cluster. The same goes for the measurements of H. Schlumbohm at $p = 1.3 - 130 \, kPa$ [67].

Also the recent measurements at $p = 1 \, kPa$ by P.M.C.C. Encarnação et al. [19] were performed without mass spectrometry. As we will see in section 4.1, this experiment too has probably measured the mobility of clusters. Intriguingly, their mobility shows a step at $E/N \approx 20 \, Td$. At higher fields, K is close to other measurements of the cluster mobility. With the exception of W.T. Huntress Jr. [31] who found a linear rise at much lower pressures, no other experiment seems to have measured the mobility below 25 Td.

A PDG-style profile plot [55] of the mobility measurements is shown in figure 3 (left). The values of A.B. Rakshit and P. Warneck are not included (see above) nor are those of G.P. Smith et al. [70] because they estimated the cluster mobility by scaling the mobility of O_3^-. Despite the difficulty of the measurement, the mobility of CO_2^+ is not more dispersed than the mobility of $CO_2^+ \cdot (CO_2)_n$. Both for the ion and for the cluster, measurements deemed accurate are outliers. The error scaling factors are $S = 1.3$ and $S = 2.3$.

In the remainder of this paper we use mobilities taken from the compilation [72].

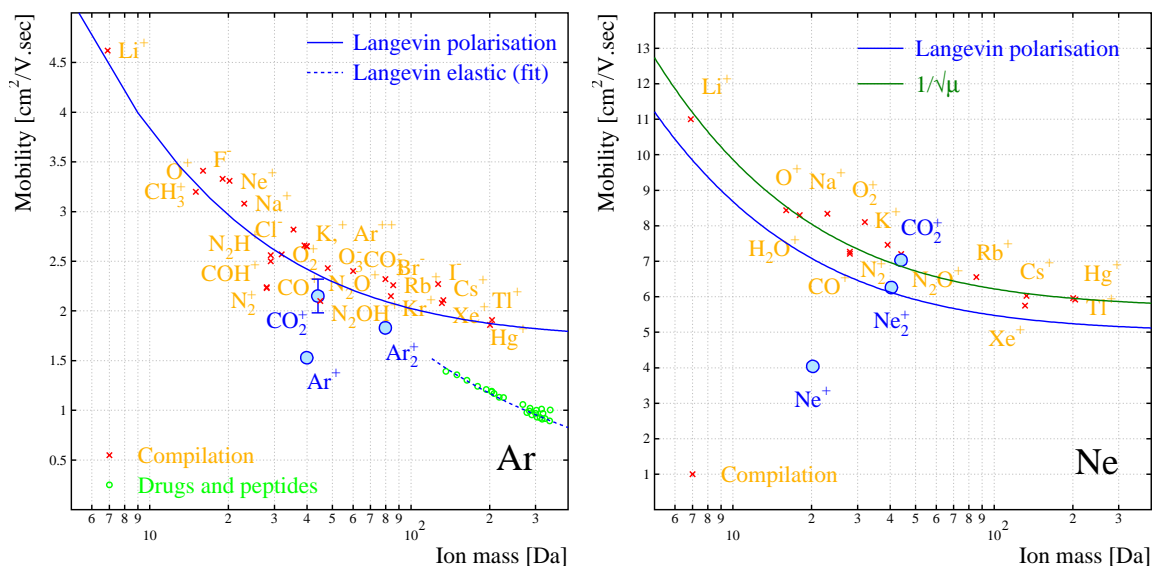## 3.4 Carbon dioxide cluster ions in argon and neon

Figure 4. Reduced mobility of ions in Ar and Ne at, or extrapolated to 10 Td. Based on: a compilation, selecting measurements at or near 300 K [15, 17, 18, 72]; measurements of aliphatic and aromatic amines at 250 °C to avoid clustering, from Zeev Karpas et al. [37]; measurements of methyl esters, at unspecified higher temperatures, from Souji Rokushika et al. [61]; and measurements of drugs and peptide compounds at 250 °C, from Laura M. Matz et al. [46]. The ions most relevant for this report are in blue, with error bars. Blue curves show the polarisation limit (solid) and the elastic limit (dashed) of the Langevin mobility formula (3.1). The curves for the elastic limit assume the masses of the ion and gas molecules are proportional to their radius cube. Manually scaled $1/\sqrt{\mu}$ hard-sphere scattering curves are in green.

The mobility of $CO_2^+ \cdot CO_2$ in Ar has to our knowledge not been measured. We therefore look for guidance from the 1905 Langevin formula [14, 38]. When the interaction between ion and gas is dominated by the charge-induced dipole force, the mobility is determined by the polarisability α. When the gas is not polarisable, or the molecules large, the Langevin formula switches to hard-sphere elastic scattering. With μ the reduced mass and d the sum of the ion and gas radii, these limits are:

$$K \propto \frac{1}{\sqrt{\alpha\mu}} \quad \ldots \quad \frac{1}{d^2\sqrt{\mu}}. \tag{3.1}$$

In principle, the Langevin formula gives absolute estimates in the polarisation limit because α is accurately known for our gases. Figure 4 shows that the mobility of ions in Ar is well described

by the polarisation limit, except that Ar^+ is slow in its parent gas due to resonant charge exchange. But the formula systematically overestimates the mobility in CO_2 by $20-25\%$, see figure 5. Scattering in CO_2 is in part inelastic because of the numerous internal degrees of freedom. This changes the mobility by 10% only, as pointed out by Edward A. Mason and Earl W. McDaniel [45]. Another factor could be the tendency of CO_2 to cluster, even though the measurements attempted to avoid clusters. The polarisation limit is not accurate in Ne either.

In the elastic limit, no absolute estimates can be made with the Langevin formula because d is not known with precision. The functional dependence on the masses is confirmed however by measurements of organic molecules. This indicates that the mobility of large clusters may be expected to be smaller than the polarisation limit would suggest.

3.5 Ions in noble gases

Most of the other mobilities we need have been measured: Ar^+ in Ar: $1.51 \pm 0.02 \, cm^2/V.s$ and Ar_2^+ in Ar: $1.83 \pm 0.02 \, cm^2/V.s$ as listed in the compilation of H.W. Ellis et al. [17]; CO_2^+ in Ar: $2.15 \pm 0.17 \, cm^2/V.s$ according to W. Lindinger and D.L. Albritton [42]; Ne^+ in Ne: $3.91 \pm 0.04 \, cm^2/V.s$, Ne_2^+ in Ne: $6.34 \pm 0.12 \, cm^2/V.s$ and CO_2^+ in Ne: $7.26 \pm 0.15 \, cm^2/V.s$ using the compilation of H.W. Ellis et al. [15, 17, 72], and taking the more recent of the estimates for Ne_2^+ [6, 52]. All mobilities are quoted for $E/N = 20 \, Td$, a typical field used for the measurements we will discuss in section 4.
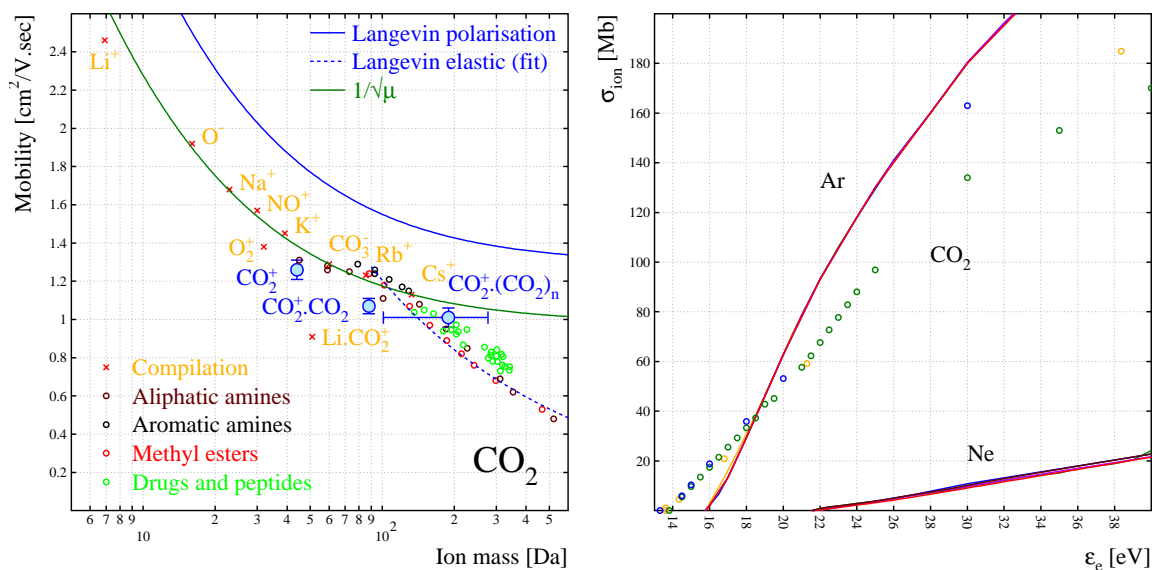

Figure 5. *Left*: reduced mobility of ions in CO_2 at, or extrapolated to 10 Td. The large horizontal error bar reflects the uncertainty in the size of $CO_2^+ \cdot (CO_2)_n$ at atmospheric pressure (section 2.5). See the caption of figure 4 for further information. *Right*: electron-impact ionisation cross sections of Ar, Ne (lines) and CO_2 (markers). Retrieved from LXCat [53] on December 19th, 2014 and February 27th, 2015. Argon databases: Magboltz 8.9 (Steve Biagi), Hayashi (Makoto Hayashi [23]), IST-Lisbon (D. Rapp and P. Englander-Golden [59]), Morgan (W. Lowell Morgan, Kinema Research Software) and Phelps (C. Yamabe et al. [74]). Neon databases: Morgan (W. Lowell Morgan, Kinema Research Software), SIGLO [48], Phelps [56], Magboltz 7.1 and 8.9 (Steve Biagi), Puech [57]. CO_2 databases: Hayashi ([54]), Itikawa (source not specified) and Morgan (W. Lowell Morgan, Kinema Research Software).
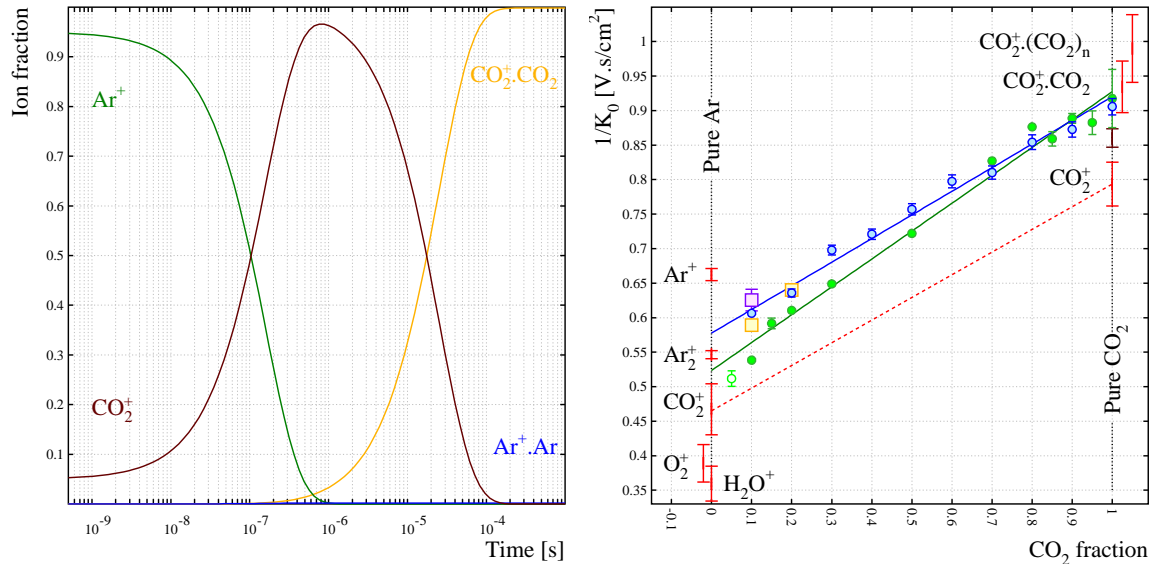
4 Experimental data

4.1 Coimbra measurement

Figure 6. *Left*: ion and cluster count as function of time at $p = 1070\,\mathrm{Pa}$. Even if 95% of the initial ions are Ar^+ hardly any $Ar^+ \cdot Ar$ is produced because Ar^+ prefers to transfer its charge to CO_2^+ at low pressure. *Right*: Blanc plot for Ar-CO_2 mixtures. Blue points are measurements by G. Schultz et al. [68]; the blue line is a linear fit to this data; green points come from P.M.C.C. Encarnação et al. [19]; the green line is a linear fit for which the light green point is not taken into account (see text); the purple point was measured in ALICE with wet gas (section 4.4), and the orange points come from an ALICE prototype chamber ("Praktikum", section 4.3); red markers and error bars are mobilities for pure gases (section 3); the red line is the mobility expected for a CO_2^+ ion; the brown error bar is the weighted average from figure 3. TPC data reduced from $999\,\mathrm{hPa}$ and $25\,^{\circ}\mathrm{C}$.

P.M.C.C. Encarnação et al. [19] have published the reduced mobility of ions in Ar-CO_2 mixtures with a CO_2 fraction ranging from 0.05 to 1. They worked at $p = 1.07\,\mathrm{kPa}$, room temperature and $E/N = 20\,\mathrm{Td}$. The same group performed such measurements in Ne-CO_2 mixtures. The ions were not positively identified for lack of a mass spectrometer.

The electron-impact ionisation cross sections at $25\,\mathrm{eV}$ of the constituent gases are $\sigma_{CO_2} = 98 \pm 3\,\mathrm{Mb}$, $\sigma_{Ar} = 130 \pm 1\,\mathrm{Mb}$ and $\sigma_{Ne} = 3.7 \pm 0.3\,\mathrm{Mb}$, see figure 5. While Ar^+ and CO_2^+ are therefore produced in quantity, there will be few Ne^+. The Ar^+ ions either transfer their charge to CO_2^+ via reaction (2.5), or form molecular ions via reaction (2.6). Charge transfer, a two-body reaction, is overwhelmingly favoured at $1.07\,\mathrm{kPa}$ and production of $Ar^+ \cdot Ar$ is insignificant, even in a mixture with 95% Ar. Charge transfer also dominates in the Ne mixtures, see section 2.2.

Converting 99% of the ions to $CO_2^+ \cdot CO_2$ clusters takes between $\sim 0.3\,\mu\mathrm{s}$ in pure CO_2 and $\sim 120\,\mu\mathrm{s}$ in a 5% CO_2 mixture (figure 6, left). Since the transit times were in the range $350 - 940\,\mu\mathrm{s}$, the data with the highest Ar percentage may be influenced by residual CO_2^+ ions. For this reason, we exclude the 5% Ar point from the fit. The fit does include the measurement at $E/N = 20\,\mathrm{Td}$ of what the authors believe to be the mobility of CO_2^+ in pure CO_2, see section 3.3.
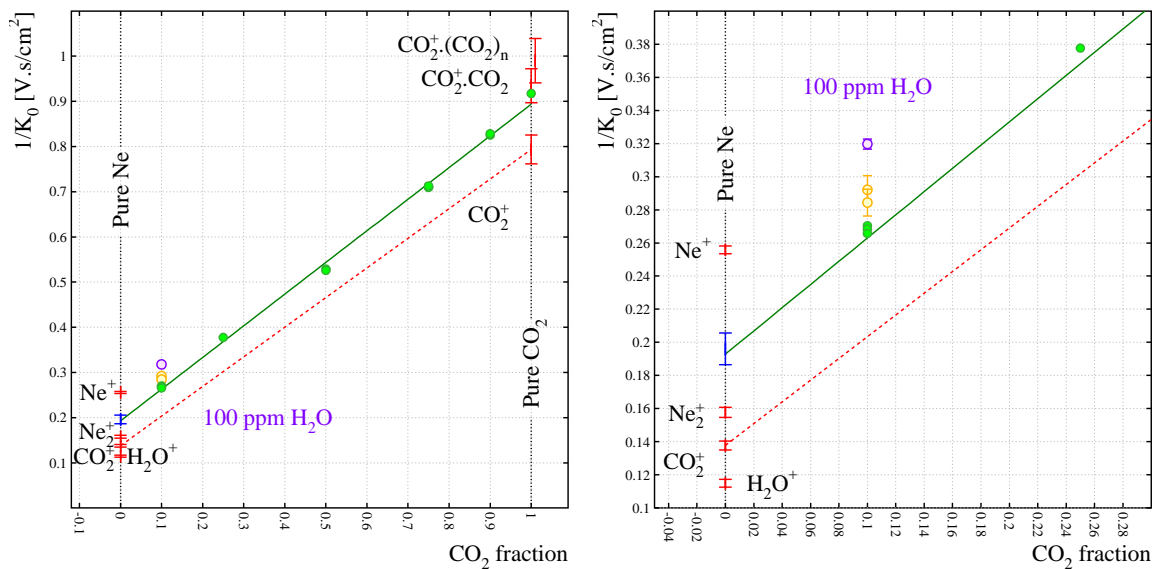
Figure 7. *Left:* Blanc diagram for Ne-CO_2 at $E/N = 20$ Td. The green points were measured in Coimbra, section 4.1. The point at 10% CO_2 suffers from lack of statistics. Orange dots (overlapping) mark the mobility observed in VTPC-1 and VTPC-2 data for the 10% mixture, reduced from 1010 hPa and 21 °C. The red line is the mobility expected for a CO_2^+ ion. The blue marker indicates the inverse mobility of a 250 Da ion in Ne, according to the polarisation limit in mass-mobility diagram 4. Also shown (purple) is the ALICE measurement in a wet gas, see section 4.4. *Right:* enlarged view.

Figure 6 (right) shows the argon Blanc plot. The measured mobility is not compatible with CO_2^+ ions, but does match $n = 1$ clusters. Since cluster growth requires higher pressure (section 2.5) large clusters should be rare here. The mobility of the $CO_2^+ \cdot CO_2$ cluster in pure Ar is not known from literature. The fit suggests $K = 1.9 \pm 0.1\,\mathrm{cm^2/V.s}$, in agreement with the Langevin formula in the polarisation limit for a 200 Da ion, see figure 4 and section 3.4. The data tend to deviate from a straight line towards pure Ar. This is probably in part due to residual CO_2^+ ions. No such trend is observed in the atmospheric pressure measurements of G. Schultz et al. discussed next.

Figure 7 is the Blanc plot for neon. Similar observations as for argon can be made, except that no deviating trend is seen for nearly pure neon.

4.2 G. Schultz et al. measurements

G. Schultz et al. [68] have measured the reduced mobility of ions in several argon-based mixtures at atmospheric pressure and room temperature. Not having a mass spectrometer, they could not identify the ions. They derived the mobility from the time an ion needs to traverse a 1.95 cm wide gap with a uniform reduced field of $E/N \leq 20$ Td, close to the reduced field used in Coimbra.

Under these conditions, formation of single clusters takes only a few ns, see figure 2 (right), while traversing the gap took ~ 1 ms. The $CO_2^+ \cdot CO_2$ clusters therefore had ample time to grow into $CO_2^+ \cdot (CO_2)_n$. By the time they arrived, they had probably already given way to H_2O and CO clusters, see section 2.5. We are not aware of measurements of the mobility of such contamination-derived clusters, but they are no doubt larger and slower than the clusters seen by P.M.C.C. Encarnação et al. [19]. This is confirmed by the Blanc diagram in figure 6 (right),
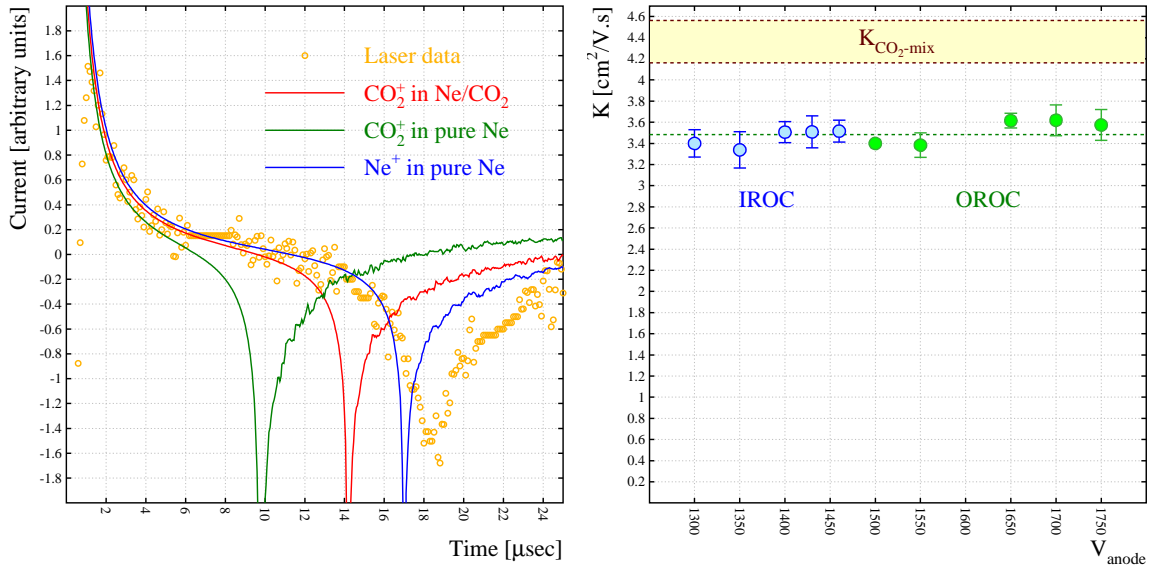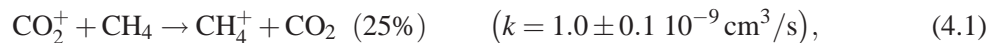
– 11 –

4.3 NA49 TPC readout chambers (dry gas)

Figure 8. *Left*: signals induced by ions moving from an anode wire to a field wire in the NA49 VTPC-1. Orange markers: laser signal shape provided by Rainer Renfordt [60]; red: signal calculated for CO_2^+ in the Ne-CO_2 mixture, using Blanc's law (4.3); green: CO_2^+ in pure Ne, neglecting the CO_2 component of the carrier gas; blue: Ne^+ in pure Ne, neglecting in addition charge exchange reactions (2.7) and (2.8). *Right*: ion mobility in the ALICE inner and outer readout chambers derived from the measured anode-cathode transit times [62]. The mobility is assumed E/N independent. The error on the data is mainly due to difficulty pinpointing the peak. The orange band shows the calculated low-field mobility for CO_2 ions, see section 4.5.

NA49 [1] had four TPCs, now used by NA61: VTPC-1, VTPC-2, MTPC-L and MTPC-R. Anode wires multiplied the ionisation electrons and pads picked up the signal induced by the moving ions and electrons. Many of the ions ended up on field wires located between the anode wires. On approach, the ions accelerated and generated a spike in the pad current. The delay between the anode and field wire spikes gives information about the ion mobility.

During data taking, the VTPCs contained Ne $90\% - CO_2$ 10% but for laser measurements of the pulse shape also Ar $90\% - CO_2$ 10% was used. The gas contained < 20 ppm humidity. The MTPCs were operated with Ar $90\% - CO_2$ $5\% - CH_4$ 5%. These mixtures fall outside the scope of the present paper because the CO_2^+ ions rapidly transfer their charge to CH_4^+ and HCO_2^+ [3] and hence are not responsible for the observed signals:

$$CO_2^+ + CH_4 \rightarrow CH_4^+ + CO_2 \ (25\%) \qquad \left(k = 1.0 \pm 0.1 \ 10^{-9} \, cm^3/s\right), \qquad (4.1)$$

$$\rightarrow HCO_2^+ + CH_3 \ (75\%). \qquad (4.2)$$

The CO_2^+ ions should form clusters both in Ne $90\% - CO_2$ 10% and in Ar $90\% - CO_2$ 10 %, see section 2. That something happens to the CO_2^+ ions can be seen in figure 8 (left) and table 1: the signal ions arrive 4.3 ± 0.5 μs (VTPC-1) or 4.7 ± 0.5 μs (VTPC-2) later than would be expected

from Blanc's law using E/N-dependent mobilities of CO_2^+ from literature [15, 72]:

$$\frac{1}{K_{CO_2^+\text{-mix}}} = \frac{0.9}{K_{CO_2^+\text{-Ne}}} + \frac{0.1}{K_{CO_2^+\text{-}CO_2}}, \qquad K_{CO_2^+\text{-mix}}^{20\,\text{Td}} = 4.91 \pm 0.20\,\text{cm}^2/\text{V.s}. \qquad (4.3)$$

Blanc's law should be accurate to 5 % for the gases and low fields used here (see section 3).

Surprisingly, the mobility of Ne^+ in Ne nearly reproduces the timing of the spike. This must be a coincidence, even if a similar near-agreement exists in the Ar 90 % $- CO_2$ 10 % data.

The E/N-dependence of the mobility can not be determined from a single time measurement. However, we can estimate the weak-field mobility $K_{\text{ion-mix}}^0$ given that the field between the anode and field wires stays in the range $5-50\,\text{Td}$ for 90 % of the way. The mobility of ions generally changes by < 10 % in this domain.

If the mobility is assumed constant, then $K_{\text{ion-mix}} \approx 3.75\,\text{cm}^2/\text{V.s}$. To have an idea of the systematic error, we repeated the approach using the shapes of Ne^+ in Ne, which falls as a function of E/N, and of CO_2^+ in Ne, which has a hump. This yields mobilities at $20\,\text{Td}$ of $\sim 3.65\,\text{cm}^2/\text{V.s}$ and $\sim 3.90\,\text{cm}^2/\text{V.s}$.
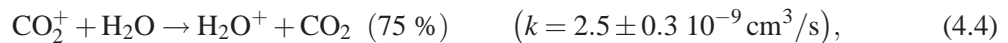
The ion responsible for the spike is therefore significantly slower than CO_2^+ would be according to (4.3). Instead, the Blanc diagram (figure 7) shows that the signal ion is compatible with being a cluster ion. Measurements in the "Praktikum" chamber filled with Ar 90 % $- CO_2$ 10 % have been included in the Blanc diagram for argon, figure 6 [60].

## 4.4 ALICE TPC inner readout chamber (wet gas)

ALICE has performed similar measurements as NA49, but using the ALICE IROC inner readout chambers [2]. These chambers have no field wire, but the arrival of the ions on the cathode wires is visible. Another difference with NA49 is that the ALICE mixture contains 100 ppm water. Water, even in trace quantities, has long been known to lower the ion mobility in some gases [21].

R.J. Munson and co-workers [13, 30, 49–51] have measured the effect of water on the transport of alkali ions in noble gases. They interpreted their observations as H_2O molecules being attracted by alkali ion charges. They emphasised that H_2O is polar and that the attraction force is therefore $\propto 1/r^3$ instead of $\propto 1/r^5$ as would be the case for an induced dipole. Even though CO_2^+, contrary to the alkali ions, will exchange charge with H_2O, the underlying mechanism should still apply for the TPC data.

The effect is also known from IMS in air, where it is used to determine the humidity level [22]. Clustering in air is thought to start with ionisation forming N_2^+ which transfers its charge to H_2O^+ which reacts with more H_2O to produce H_3O^+. In our gas mixtures, these steps are replaced by electron or proton exchange between CO_2^+ and H_2O:

$$CO_2^+ + H_2O \rightarrow H_2O^+ + CO_2 \;\; (75\text{ %}) \qquad \left(k = 2.5 \pm 0.3\ 10^{-9}\,\text{cm}^3/\text{s}\right), \qquad (4.4)$$
$$\rightarrow HCO_2^+ + OH \;\; (25\text{ %}). \qquad (4.5)$$

H_3O^+ results from a reaction with another H_2O molecule:

$$HCO_2^+ + H_2O \rightarrow H_3O^+ + CO_2 \qquad \left(k = 2.8 \pm 0.7\ 10^{-9}\,\text{cm}^3/\text{s}\right). \qquad (4.6)$$
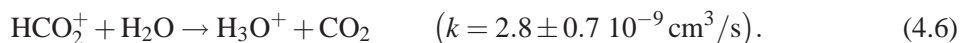
In the presence of 100 ppm water, both reactions have a characteristic time of $0.15-0.16\ \mu\text{s}$ [3]. This is three orders of magnitude slower than clustering reaction (2.10). We must therefore assume

that reaction (4.5) also takes place with $CO_2^+ \cdot (CO_2)_n$ clusters in formation. As pointed out by Kenzo Hiraoka, H_3O^+ forms strong hydrogen bonds with a very large number of H_2O molecules, resulting in an extended $H^+ \cdot (H_2O)_n$ network [25].

Water clusters with a size around 20 have been reported at 120 K, but at room temperature the most common size is $n \approx 5$ [39, 41]. We speculate that water molecules, taking advantage of their polarity, attach themselves to CO_2-based clusters, forming mixed (protonated) clusters [24, 36]. Thus, water clusters are arguably larger and slower than $CO_2^+ \cdot CO_2$ clusters produced in dry gas, but the latter grow with time (section 2.5).

Assuming a constant mobility as for the NA49 data, the measured transit time translates to $K_{\text{ion-mix}} = 3.40 \pm 0.03\,\text{cm}^2/\text{V.s}$ in Ne 90 %/CO_2 10 %. This is indeed smaller than we found for dry gas (section 4.3). The same trend is observed in Ar 90 %/CO_2 10 %, see the Blanc diagrams figures 6 and 7 and table 1. The difference of 10 % is perhaps even larger than expected from literature. $K_{\text{ion-mix}}$ is a fortiori smaller than Blanc's law predicts in the absence of clustering.

Table 1. Measured ion transit time t_{exp} from the anode wires to the field or cathode wires, in the NA49 and ALICE readout chambers, extracted from signal shapes such as figure 8. Also listed are t_{mix}, the time CO_2^+ ions are expected to take in the gas mixture according to Blanc's law (4.3) and t_{fixed}, the time needed at constant mobility $K = 1\,\text{cm}^2/\text{V.s}$. The calculated times have a systematic uncertainty of ~ 2 % and a statistical uncertainty < 1 %. The IROC measurements were done for this paper. The third line is based on figure 15 from [1], erroneously labeled MTPC data in the publication. Other data is from Rainer Renfordt [60].

TPC	V_{anode} [V]	Drift gas	H_2O [ppm]	t_{exp} [μs]	t_{mix} [μs]	t_{fixed} [μs]	K [cm^2/V.s]
VTPC-1	1110	Ne 90 %/CO_2 10 %	< 20	18.5 ± 0.5	14.2	68.2	3.7 ± 0.1
VTPC-2	970	Ne 90 %/CO_2 10 %	< 20	22.5 ± 0.5	17.8	84.9	3.8 ± 0.1
VTPC-2	970	Ne 90 %/CO_2 10 %	< 20	22.3 ± 0.5	17.8	84.9	3.8 ± 0.1
IROC	1263	Ne 90 %/CO_2 10 %	100	25.7 ± 0.2	18.2	87.4	3.40 ± 0.03
Praktikum	1250	Ar 90 %/CO_2 10 %	< 20	63.6 ± 0.5	59.7	119.6	1.88 ± 0.01
IROC	1327	Ar 90 %/CO_2 10 %	100	47 ± 1	41.5	83.1	1.77 ± 0.04
Praktikum	1453	Ar 80 %/CO_2 20 %	< 20	59.6 ± 0.5	54.7	102.9	1.72 ± 0.01

## 4.5 ALICE TPC readout chambers (nitrogen gas)

S. Rossegger and W. Riegler have measured the anode-cathode transit time in the ALICE TPC filled with Ne 85.7 % $-$ CO_2 9.5 % $-$ N_2 4.8 % [62]. All constituents of the mixture are ionised in avalanches. Ne^+ reacts primarily with CO_2 via reactions (2.7) and (2.8) in $\tau \sim 8$ ns. Ne^+ can also form dimers via reaction (2.9) but this is less likely given that $\tau = 38$ ns. Charge transfer to N_2 is insignificant with $\tau = 7.7\,\mu$s [3]:

$$Ne^+ + N_2 \rightarrow Ne + N_2^+ \qquad \left(k = 1.1\ 10^{-13}\,\text{cm}^3/\text{s} \right). \tag{4.7}$$

N_2^+ more likely transfers its charge in 0.78 ns to CO_2 [3]:

$$N_2^+ + CO_2 \rightarrow N_2 + CO_2^+ \qquad \left(k = 5.5\ 10^{-10}\,\text{cm}^3/\text{s} \right). \tag{4.8}$$
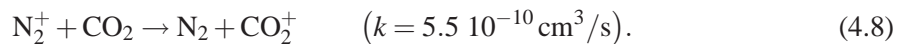
Nitrogen dimers are almost not formed since $\tau = 12\,\text{ns}$ [69]:

$$N_2^+ + 2N_2 \rightarrow N_2^+ \cdot N_2 + N_2 \qquad \left(k = 0.6\ 10^{-28}\,\text{cm}^6/\text{s}\right). \tag{4.9}$$
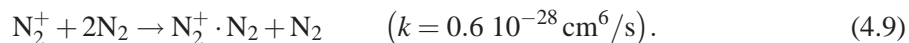
Hence, only CO_2^+ ions remain after $10\,\text{ns}$, a delay that is insignificant compared with the transit time which is of the order of $20\,\mu\text{s}$. CO_2 is the component with the lowest ionisation potential and is expected only to cluster with itself, as in the mixtures discussed earlier.

That clustering indeed occurs can be seen by comparing the calculated mobility of CO_2^+ ions in the mixture:

$$\frac{1}{K_{CO_2^+\text{-mix}}} = \frac{0.857}{K_{CO_2^+\text{-Ne}}} + \frac{0.095}{K_{CO_2^+\text{-CO}_2}} + \frac{0.048}{K_{CO_2^+\text{-N}_2}}, \qquad K_{CO_2^+\text{-mix}}^{20\,\text{Td}} = 4.64 \pm 0.20\,\text{cm}^2/\text{V.s} \tag{4.10}$$

with the (constant) mobility that best fits the measurements, $K_{\text{ion-mix}} = 3.49 \pm 0.03\,\text{cm}^2/\text{V.s}$, see figure 8 (right). The mobility in these chambers is lower than in NA49 because of the smaller Ne fraction and the presence of N_2. The cluster-induced reduction of the mobility is $20-25\,\%$, similar to what we found for NA49 in section 4.3.

5 Conclusion

According to the literature on ion-molecule reactions, the signal ions in CO_2-quenched mixtures of Ar and Ne are $CO_2^+(CO_2)_n$ cluster ions, not CO_2^+ or noble gas ions. Experimental evidence confirms this. Cluster ions are heavier and slower than CO_2^+ ions. Their mobility in Ar-CO_2 and Ne-CO_2 mixtures can be calculated from Blanc's law. Water reduces the ion mobility in these mixtures. Mass spectrometry is key to a better understanding of the behaviour of ions in detectors.

Acknowledgments

References

[1] NA49 collaboration, S. Afanasev et al., *The NA49 large acceptance hadron detector*, *Nucl. Instrum. Meth.* **A 430** (1999) 210.

[2] J. Alme et al., *The ALICE TPC, a large 3-dimensional tracking device with fast readout for ultra-high multiplicity events*, *Nucl. Instrum. Meth.* **A 622** (2010) 316 [arXiv:1001.1950].

[3] V.G. Anicich and W.T. Huntress Jr., *A survey of bimolecular ion-molecule reactions for use in modeling the chemistry of planetary atmospheres, cometary comae, and interstellar clouds*, *Astrophys. J. Suppl.* **62** (1986) 553.

[4] V.G. Anicich, *Evaluated Bimolecular Ion-Molecule Gas Phase Kinetics of Positive Ions for Use in Modeling Planetary Atmospheres, Cometary Comae, and Interstellar Clouds*, *J. Phys. Chem. Ref. Data* **22** (1993) 1469.

[5] E. Basurto et al., *Mobility of* He^+, Ne^+, Ar^+, N_2^+, O_2^+, *and* CO_2^+ *in their parent gas*, *Phys. Rev.* **E 61** (2000) 3053.

[6] E.C. Beaty and P.L. Patterson, *Mobilities and Reaction Rates of Neon Ions in Neon*, *Phys. Rev.* **170** (1968) 116.

[7] Z. Berant et al., *Effects of temperature and clustering on mobility of ions in carbon dioxide*, *J. Phys. Chem.* **93** (1989) 7529.

[8] S.F. Biagi, *Monte Carlo simulation of electron drift and diffusion in counting gases under the influence of electric and magnetic fields*, *Nucl. Instrum. Meth.* **A 421** (1999) 234.

[9] M.A. Biondi and L.M. Chanin, *Blanc's Law — Ion Mobilities in Helium-Neon Mixtures*, *Phys. Rev.* **122** (1961) 843.

[10] A. Blanc, *Recherches sur les mobilités des ions dans les gaz*, *J. Phys. Theor. Appl.* **7** (1908) 825.

[11] P. Coxon and J.L. Moruzzi, *Ion-molecule reactions in* CO_2 *and* CO_2-CO *mixtures*, *J. Phys.* **D 10** (1977) 969.

[12] P.A. Coxon and J.L. Moruzzi, *Positive ion mobilities in carbon dioxide*, *J. Phys. Colloques* **40** (1979) C7-117.

[13] H.G. David and R.J. Munson, *The Mobility of Alkali Ions in Gases. IV. Measurements in Gaseous Mixtures*, *Proc. Roy. Soc. Lond.* **A 177** (1941) 192.

[14] P.G. Davies et al., *Critical Review*, *Phil. Trans. Roy. Soc. Lond.* **A 259** (1966) 302.

[15] H.W. Ellis et al., *Transport properties of gaseous ions over a wide energy range. Part II*, *At. Data Nucl. Data tables* **22** (1978) 179.

[16] H.W. Ellis et al., *Ion identity and transport properties in* CO_2 *over a wide pressure range*, *J. Chem. Phys.* **64** (1976) 3935.

[17] H.W. Ellis et al., *Transport properties of gaseous ions over a wide energy range*, *At. Data Nucl. Data tables* **17** (1976) 177.

[18] H.W. Ellis et al., *Transport properties of gaseous ions over a wide energy range. Part III*, *At. Data Nucl. Data tables* **31** (1984) 113.

[19] P.M.C.C. Encarnação et al., *Experimental Ion Mobility measurements in* Ar-CO_2 *mixtures*, 2015 *JINST* **10** P01010.

[20] P.C. Engelking, *Determination of cluster binding energy from evaporative lifetime and average kinetic energy release: Application to* $(CO_2)_n^+$ *and* Ar_n^+ *clusters*, *J. Chem. Phys.* **87** (1987) 936.

[21] H.A. Erikson, *On The Effect of the Medium on Gas Ion Mobility*, *Phys. Rev.* **30** (1927) 339.

[22] B.C. Hauck et al., *Determining the water content of a drift gas using reduced ion mobility measurements*, *Int. J. Mass Spectrom.* **368** (2014) 37.

[23] M. Hayashi, *Bibliography of Electron and Photon Cross sections with Atoms and Molecules Published in the 20th Century — Argon*, NIFS-DATA-72, Toki, Japan (2003).

[24] K. Hiraoka et al., *Stability and structure of cluster ions in the gas phase: Carbon dioxide with* Cl^-, H_3O^+, HCO_2^+, *and* HCO^+, *J. Chem. Phys.* **84** (1986) 2091.

[25] K. Hiraoka, *Fundamentals of Mass Spectrometry*, Springer Science & Business Media, New York, U.S.A. (2013), pg. 135.

[26] K. Hiraoka and T. Mori, *Formation and stabilities of cluster ions* Ar_n^+, *J. Chem. Phys.* **90** (1989) 7143.

[27] K. Hiraoka et al., *Determination of the stabilities of* $CO_2^+ \cdot (CO_2)_n$ *and* $O_2^+ \cdot (CO_2)_n$ *clusters with* $n = 1 - 6$, *Chem. Phys. Lett.* **146** (1988) 535.

[28] T. Holstein, *Mobility of Positive Ions in Gas Mixtures*, abstract of paper B6 in *Abstracts of Papers Presented at the Eighth Annual Gaseous Electronics Conference Held at Schenectady, New York, October 20–22, 1955*, *Phys. Rev.* **100** (1955) 1230. Complete paper not found. See [9].

[29] J. Hornbeck, *The Drift Velocities of Molecular and Atomic Ions in Helium, Neon, and Argon*, *Phys. Rev.* **84** (1951) 615.

[30] K. Hoselitz, *The Mobility of Alkali Ions in Gases. V. Temperature Measurements in the Inert Gases*, *Proc. Roy. Soc. Lond.* **A 177** (1941) 200.

[31] W.T. Huntress Jr., *Ion Cyclotron Resonance Power Absorption: Collision Frequencies for* CO_2^+, N_2^+, *and* H_3^+ *Ions in Their Parent Gases*, *J. Chem. Phys.* **55** (1971) 2146.

[32] Y. Ikezoe et al., *Gas Phase Ion-Molecule Reaction Rate Constants Through 1986*, Maruzen Company Ltd, Tokyo, Japan (1987).

[33] Y. Ikezoe et al., *Ions in carbon dioxide at an atmospheric pressure*, *Radiat. Phys. Chem.* **20** (1982) 253.

[34] A.J. Illies, *Thermochemistry for the gas-phase ion-molecule clustering of* $CO_2^+CO_2$, $SO_2^+CO_2$, $N_2O^+N_2O$, $O_2^+CO_2$, NO^+CO_2, $O_2^+N_2O$ *and* NO^+N_2O: *description of a new hybrid drift tube/ion source with coaxial electron beam and ion exit apertures*, *J. Phys. Chem.* **92** (1988) 2889.

[35] A.J. Illies et al., *Photoinduced Intramolecular Charge Transfer: Photodissociation of* $CO_2^+ \cdot Ar$ *Cluster Ions*, *J. Am. Chem. Soc.* **107** (1985) 2842.

[36] Y. Inokuchi et al., *Structures of water-CO_2 and methanol-CO_2 cluster ions:* $[H_2O \cdot (CO_2)_n]^+$ *and* $[CH_3OH \cdot (CO_2)_n]^+$ ($n = 1 - 7$), *The J. Chem. Phys.* **130** (2009) 154304.

[37] Z. Karpas et al., *Effect of temperature on the mobility of ions*, *J. Am. Chem. Soc.* **111** (1989) 6015.

[38] M.P. Langevin, *Une formule fondamentale de théorie cinétique*, *Ann. Chem. Phys.* **5** (1905) 245.

[39] Y.K. Lau et al., *Thermodynamics and kinetics of the gas-phase reactions* $H_3O^+(H_2O)_{n-1} + water = H_3O^+(H_2O)_n$, *J. Am. Chem. Soc.* **104** (1982) 1462.

[40] V. Lepère et al., *Lifetime and yield of metastable* Ar_2^+ *ions*, *J. Chem. Phys.* **123** (2005) 174307.

[41] A. Likholyot, *Experimental and Theoretical Study of Ionic Clustering Reactions Involving Water*, Ph.D. Thesis, Eidgenössische Technische Hochschule Zürich, Switzerland, (2000).

[42] W. Lindinger and D.L. Albritton, *Mobilities of various mass-identified positive ions in helium and argon*, *J. Chem. Phys.* **62** (1975) 3517.

[43] W.F. Liu and D.C. Conway, *Ion-molecule reactions in* Ar *at 296, 195, and 77 K*, *J. Chem. Phys.* **62** (1975) 3070.

[44] P.M. Martin, *Handbook of Deposition Technologies for Films and Coatings: Science, Applications and Technology*, chapter 2, W. Andrew ed., Elsevier (2010), p. 43. Book seen via Google, refers to [32].

[45] E.A. Mason and E.W. McDaniel, *Transport properties of ions in gases*, John Wiley & Sons, (1988), chapter 6-1 F, pg. 259–262.

[46] L.M. Matz et al., *Investigation of drift gas selectivity in high resolution ion mobility spectrometry with mass spectrometry detection*, *J. Am. Soc. Mass Spectrom.* **13** (2002) 300.

[47] M.M. Meot-Ner (Mautner) and S.G. Lias, *Binding Energies Between Ions and Molecules, and The Thermochemistry of Cluster Ions*, in *NIST Chemistry WebBook*, NIST Standard Reference Database Number 69, P.J. Linstrom and W.G. Mallard eds., National Institute of Standards and Technology, Gaithersburg MD, 20899, retrieved 4 May 2015.

[48] J. Meunier et al., *Numerical model of an ac plasma display panel cell in neon-xenon mixtures*, *J. Appl. Phys.* **78** (1995) 731.

[49] R.J. Munson, *The Mobility of Alkali Ions in Gases. III. The Mobility of Alkali Ions in Water Vapour*, *Proc. Roy. Soc. Lond.* **A 172** (1939) 51.

[50] R.J. Munson and K. Hoselitz, *The Mobility of Alkali Ions in Gases. II. The Attachment of Inert Gas Atoms to Alkali Ions*, *Proc. Roy. Soc. Lond.* **A 172** (1939) 43.

[51] R.J. Munson and A.M. Tyndall, *The Mobility of Alkali Ions in Gases. I. The Attachment of Water Molecules to Alkali Ions in Gases*, *Proc. Roy. Soc. Lond.* **172** (1939) 28.

[52] O.J. Orient, *Mobility of mass-identified ions in neon and reaction rate coefficient for* $Ne^+ + 2Ne \rightarrow Ne_2^+ + Ne$, *Chem. Phys. Lett.* **23** (1973) 579.

[53] L.C. Pitchford et al., *LXCat, a web-based, community-wide project on data needed in modeling low temperature plasmas*, www.lxcat.net.

[54] L.C. Pitchford eds., *Swarm Studies and Inelastic Electron-Molecule Collisions*, *Proceedings of the Meeting of the Fourth International Swarm Seminar and the Inelastic Electron-Molecule Collisions Symposium*, Springer-Verlag, Tahoe City, California, U.S.A., 19–23 July 1985,

[55] PARTICLE DATA GROUP collaboration, K.A. Olive, *Review of Particle Physics*, *Chin. Phys.* **C 38** (2014) 14.

[56] A.V. Phelps, *A compilation of atomic and molecular data*, assembled and evaluated by A.V. Phelps and collaborators, http://jilawww.colorado.edu/∼avp/, last updated in 2010.

[57] V. Puech and S. Mizzi, *Collision cross sections and transport parameters in neon and xenon*, *J. Phys.* **D 24** (1991) 1974.

[58] A.B. Rakshit and P. Warneck, *Rate Coefficients and Product Ion Distributions for Reactions of* $CO_2 \cdot CO_2^+$ *Ions with Neutral Molecules at* 300 K, *Z. Naturforsch.* **34a** (1979) 1410. Erratum (it does not concern the mobilities): http://www.znaturforsch.com/aa/v35a/35a0256.pdf.

[59] D. Rapp and P. Englander-Golden, *Total Cross sections for Ionization and Attachment in Gases by Electron Impact. I. Positive Ionization*, *J. Chem. Phys.* **43** (1965) 1464.

[60] R. Renfordt, private communication, data taken in 1998, communicated in 1999 and 2014.

[61] S. Rokushika et al., *Ion mobility spectrometry in carbon dioxide*, *Anal. Chem.* **58** (1986) 361.

[62] S. Rossegger and W. Riegler, *Signal shapes in a TPC wire chamber*, *Nucl. Instrum. Meth.* **A 623** (2010) 927.

[63] Ö. Şahin, private communication, (2015).

[64] S.I. Sandler and E.A. Mason, *Kinetic-Theory Deviations from Blanc's Law of Ion Mobilities*, *J. Chem. Phys.* **48** (1968) 2873.

[65] M. Saporoschenko, *Drift Velocities of* O_2^+, CO_2^+, *and* CO_4^+ *Ions in* CO_2 *Gas*, *Phys. Rev.* **A 8** (1973) 1044.

[66] S.M. Schildcrout et al., *Mass Spectrometric Study of Ion-Neutral Reactions in Radio-Frequency Discharges in Carbon Dioxide*, *J. Chem. Phys.* **52** (1970) 5767.

[67] H. Schlumbohm, *Elektronenlawinen in elektronegativen Gasen*, *Z. Phys.* **166** (1962) 192.

[68] G. Schultz et al., *Mobilities of positive ions in some gas mixtures used in proportional and drift chambers*, *Rev. Phys. Appl. (Paris)* **12** (1977) 67.

[69] B.M. Smirnov, *Cluster Ions and Van der Waals Molecules*, Gordon and Breach Science Publishers, (1992).

[70] G.P. Smith et al., *Photodissociation of atmospheric positive ions. I.* $5300 - 6700\,\text{Å}$, *J. Chem. Phys.* **67** (1977) 3818.

[71] D.L. Turner and D.C. Conway, *Study of the* $2Ar + Ar_2^+ = Ar + Ar_3^+$ *reaction*, *J. Chem. Phys.* **71** (1979) 1899.

[72] L.A. Viehland and E.A. Mason, *Transport Properties of Gaseous Ions over a Wide Energy Range, IV*, *At. Data Nucl. Data tables* **60** (1995) 37.

[73] Wolfram Research Inc., *Mathematica*, version 10.6, (2014).

[74] C. Yamabe et al., *Measurement of free-free emission from low-energy-electron collisions with* Ar, *Phys. Rev.* **A 27** (1983) 1345.